Available online at www.sciencedirect.com
ScienceDirect
Mathematical Biosciences xxx (2006) xxx–xxx
Mathematical Biosciences
www.elsevier.com/locate/mbs

Frequency-dependent response properties of adapting spiking neurons

Guido Gigante [a,b,*], Paolo Del Giudice [b], Maurizio Mattia [b]

[a] *Department of Physics, University of Rome "La Sapienza", P.le Aldo Moro 5, 00185 Roma, Italy*
[b] *Complex System Unit, Technologies and Health Department, Istituto Superiore di Sanità – V.le Regina Elena 299, 00161 Roma, Italy*

Received 1 June 2006; received in revised form 22 October 2006; accepted 15 November 2006

Abstract

The dynamics of a population of integrate and fire (IF) neurons with spike-frequency adaptation (SFA) is studied. Using a population density approach and assuming a slow dynamics for the variable driving SFA, an equation for the emission rate of a finite set of uncoupled neurons is derived. The system dynamics is then analyzed in the neighborhood of its stable fixed points by linearizing the emission rate equation. The information transfer properties are then probed by perturbing the system with a sinusoidal input current: despite the low-pass properties of the dynamical variable associated with SFA, the adapting IF neuron behaves as a band-pass device and a phase-lock condition appears at a frequency related to the characteristic time constants of both neuronal and SFA dynamics. When a finite set of neurons is considered, the power spectral density of the pooled firing rates shows for intermediate ω a rich pattern of resonances. Theoretical predictions are successfully compared to numerical simulations.

Keywords: Spike-frequency adaptation; Stochastic modelling; Resonant properties

* Corresponding author. Tel.: +39 06 49902513; fax: +39 06 49387075.
E-mail address: guido.gigante@iss.infn.it (G. Gigante).

0025-5564/$ - see front matter © 2006 Elsevier Inc. All rights reserved.
doi:10.1016/j.mbs.2006.11.010

1. Introduction

A neuron lowers its firing rate upon receiving sustained stimulation. This behavior, customarily termed spike-frequency adaptation (SFA in the following), is pervasively observed, and is thought to be subserved by complex mechanisms involving several ionic species and characteristic time scales.

As a first step towards modelling SFA, the so called I_{AHP} (after-hyperpolarization current) scheme is adopted, by which a calcium-gated potassium current temporarily hyperpolarizes the neuron upon spike emission, with a recovery time of the order of hundreds of milliseconds. Including SFA in integrate and fire (IF) neuron models brings a host of interesting implications, both at the single neuron and the network level [1–4].

We approach the dynamics of adapting IF neurons starting from a population density approach [5,6], applying it to a finite set of non-interacting neurons through the formalism introduced in [6,7], which provides an "emission rate equation" for the time-dependent firing rate of the neurons, and incorporating SFA via an adiabatic approximation.

The behavior of the system is investigated in the neighborhood of its stable fixed points, by linearizing the emission rate equation, and the power spectral density of the neurons firing rate is computed, exhibiting a non-trivial pattern of resonances.

The information transfer properties of the adapting neuron are then analyzed; specifically, we derive from the theory the phase-locking properties which have been experimentally observed and described through a phenomenological model in [3].

2. Theoretical framework

The standard IF neuron model is endowed with an extra (inhibitory) potassium input current, proportional to the instantaneous calcium concentration c through a (potassium) conductance g. In turn, c undergoes an upward jump α upon spike emission, after which it decays with a characteristic time τ_c:

$$\begin{cases} \frac{\mathrm{d}v}{\mathrm{d}t} = -f(v) - gc + I_{\mathrm{ext}} \\ \frac{\mathrm{d}c}{\mathrm{d}t} = -\frac{c}{\tau_c} + \alpha \sum_k \delta(t - t_k) \end{cases} \tag{2.1}$$

The input external current I_{ext} is assumed to be a Gaussian memoryless noise with infinitesimal moments μ_{ext} and σ^2_{ext}, which may depend on time. I_{ext} models both the barrage of external spikes received by the neuron, as argued in the next subsection, and an externally injected deterministic current, as in a hypothetical patch-clamp experiment. t_k is the time of the kth spike emitted when the membrane potential v crosses a threshold θ and is instantaneously reset to the reset potential $v \equiv H$. In what follows we use as the model neuron the VLSI integrate and fire neuron (VIF) introduced in [8,9] with a reflecting barrier in $v = 0$ and a constant decay term ($f(v) = \beta$). The collective behavior of interacting VIF neurons has been shown to be similar to those of other IF neurons [9,6].

Fig. 1 shows an example time evolution of v and c. As the external current is turned on at $t = 0$, the calcium concentration c increases, and correspondingly the firing rate of the neuron adapts to a lower value with larger inter-spike intervals (ISI). After a transient period c fluctuates around an asymptotic constant value.

Please cite this article in press as: G. Gigante et al., Frequency-dependent response properties ..., Math. Biosci. (2006), doi:10.1016/j.mbs.2006.11.010

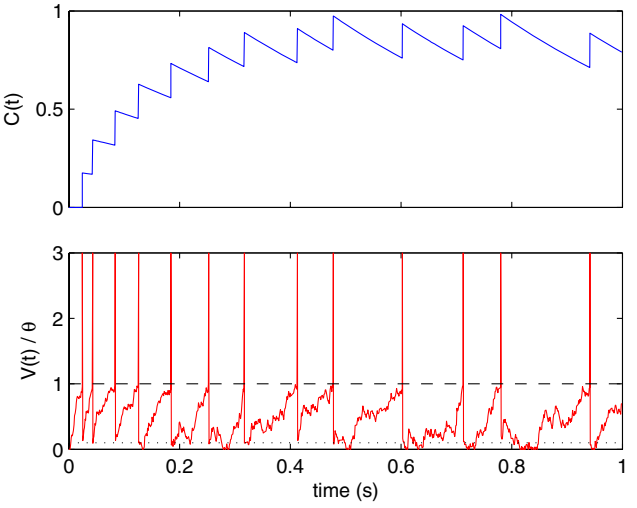

Fig. 1. Numerical integration of Eq. (2.1) for a VIF neuron with SFA receiving at $t = 0$ a noisy afferent current. The parameters set is $\beta = 1\theta$/s, $H = 0.1\theta$, $\mu_{ext} = 10\theta$/s, $\sigma^2_{ext} = 0.5\theta^2$/s, $g = 10\theta$/s, $\tau_c = 0.5$ s and $\alpha = 0.175$, where the calcium concentration is expressed in arbitrary units.

2.1. The population density approach

Each neuron in the neocortex receives, and projects, a huge number of synaptic contacts, of order some thousands. It is also found experimentally that each pre-synaptic spike induces a small change in the post-synaptic membrane potential, compared to the available dynamic range $\theta - H$. In other words, many afferent spikes are needed in order to depolarize v above the threshold θ and to provoke the emission of a spike (see for instance [10]).

Such small 'efficacy' of each single synapse allows one, in a first approximation, to consider as uncorrelated the activity of any two neurons, as their mutual influence will be very weak. The independence of spike trains from different neurons and the large number of synaptic contacts, allow then to approximate the barrage of incoming spikes with a Poisson process, possibly non-homogenous in time.

Furthermore, under physiological conditions neurons fire on average few spikes per seconds, but due to the large number of afferents the whole incoming Poisson process will have an instantaneous frequency parameter of several thousands Hz. Single neurons integrate the current due to those incoming spikes with a membrane potential time constant of order tens of ms. Since in this time window the membrane potential integrates tens of spikes or more, standard probability arguments allow us to model the input current I_{ext} as a gaussian white noise with infinitesimal mean μ_{ext} and variance σ^2_{ext}, which depend both on the total input firing rate and the synaptic efficacies (diffusion approximation) [10].

Here we assume an instantaneous synaptic transmission of the afferent spikes, which is a good approximation for AMPA and GABA receptor dynamics [11], while we neglect the non-instantaneous synaptic transmission mediated by NMDA receptors; this is justified as long as the average membrane potential is low enough to make the removal of the magnesium block unlikely, which is the case for moderate activity regimes [12].

Please cite this article in press as: G. Gigante et al., Frequency-dependent response properties ..., Math. Biosci. (2006), doi:10.1016/j.mbs.2006.11.010

Since we describe the incoming current I_{ext} as a stochastic process, Eq. (2.1) is a bi-dimensional Langevin equation, and the dynamics of the probability density function (*p.d.f.*) $p(v,c,t)$ is given by the deterministic continuity equation:

$$\partial_t p(v,c,t) = -\nabla \cdot \mathbf{S}(v,c,t)$$

where $\mathbf{S}(v,c,t)$ is the flux vector of realizations moving from (v,c) at time t, and $\nabla = \{\partial_v, \partial_c\}$. In the diffusion limit in which I_{ext} is a gaussian white noise, the above equation reduces to the following Fokker–Planck (FP) bi-dimensional equation:

$$\partial_t p(v,c,t) = \partial_c \frac{c}{\tau_c} p(v,c,t) - \partial_v \mu(v,c,t) p(v,c,t) + \frac{1}{2}\sigma^2 \partial_v^2 p(v,c,t) \tag{2.2}$$

where, in our uncoupled neuron case, $\mu(v,c,t) \doteq -f(v) - g\,c + \mu_{\text{ext}}(t)$ and $\sigma^2 \doteq \sigma^2_{\text{ext}}$ are the infinitesimal moments of v. The FP equation is complemented by the following boundary conditions: (i) an absorbing barrier at $v = \theta$, where a realization disappears upon spike emission; (ii) a reflecting barrier providing a lower bound for v ($v \geqslant 0$ for VIF neurons); (iii) a source of realizations enforcing the conservation of the probability flux, such that realizations disappeared in θ reappear in $v = H$, the reset potential, after the emission of an action potential, increasing c by α.

At a given time the histogram of the membrane potential of the different neurons in the population can be seen as a sample of the probability density function $p(v,c,t)$. The FP Eq. (2.2) may be then interpreted as the dynamics of a population of uncoupled neurons with afferent currents sharing the same statistics.

The time-dependent variable of interest will be the total emission rate per neuron $\nu(t)$:

$$\nu(t) = \int_0^\infty \nu(c,t)\mathrm{d}c \tag{2.3}$$

where $\nu(c,t)$ is the firing rate density per neuron, for an instantaneous calcium concentration c, provided by the flux component parallel to the v direction:

$$\begin{aligned}\nu(c,t) &= \{\mathbf{S}(\theta,c,t)\}_v = \mu(v,c,t)p(v,c,t) - \frac{1}{2}\sigma^2 \partial_v p(v,c,t)|_{v=\theta} \\ &= -\frac{1}{2}\sigma^2 \partial_v p(v,c,t)|_{v=\theta}\end{aligned}$$

We set $p(\theta,c,t) = 0$ since $v = \theta$ is an absorbing barrier.

Fig. 2 shows an example of the asymptotic p.d.f. $p(v,c,t)$ in the phase plane (v,c). It is seen that $p(v,c,t)$ spans a wide region in both dimensions (v,c), such that naive strategies for dimensional reduction of the problem, valid when the p.d.f. is very concentrated in one or more dimensions, are unlikely to be effective in the case shown.

2.2. Dimensional reduction: the adiabatic approximation

In order to effectively tackle the problem of solving Eq. (2.2) with its boundary conditions, we exploit the great difference of the time scales of the membrane potential and the calcium concentration dynamics, and invoke an adiabatic approximation to reduce the dimensionality of the problem.

Please cite this article in press as: G. Gigante et al., Frequency-dependent response properties ..., Math. Biosci. (2006), doi:10.1016/j.mbs.2006.11.010

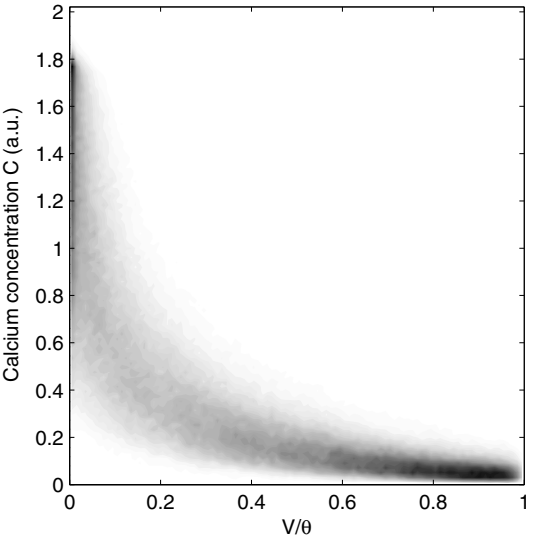

Fig. 2. Asymptotic p.d.f. $p(v, c, t)$ estimated from the numeric integration of Eq. (2.1) over 50 s after a transient period of 1 s needed to forget initial conditions. Darker regions are associated to higher probability densities, white areas correspond to $p(v, c, t) = 0$. The parameters set is the same as in Fig. 1 with the following exceptions: $H = 0$, $\mu_{\text{ext}} = 9\ \theta/\text{s}$, $\tau_c = 50$ ms and $\alpha = 1.75$.

As τ_c is supposed to be much longer than the other time scales in the system (membrane time constants, average inter-spike interval), the calcium concentration for each neuron is a very efficient integrator filtering almost all the fluctuations in the single neuron activity. Eq. (2.1) for $c(t)$ can be then well approximated by its average on a time window much smaller than τ_c:

$$\dot{c}(t) = -\frac{c(t)}{\tau_c} + \alpha v(t) \tag{2.4}$$

Furthermore, since the dynamics of c is slow, in the time between two consecutive spike emissions each neuron sees an approximately constant $I_{\text{AHP}} = -gc(t)$.

Such approximation can be better understood considering, in stationary conditions, the relative width of the $c(t)$ marginal distribution. Consider the case study of a Poissonian emitted spike train with frequency v. Both the average and the variance of $c(t)$ can be computed and are respectively $\alpha v \tau_c$ and $\alpha^2 v\ \tau_c/2$. The coefficient of variation, given by the ratio between standard deviation and mean, is then proportional to $1/\sqrt{v\tau_c}$. A constant I_{AHP} during an ISI is then a good assumption provided that $\tau_c \gg 1/v$. Such a "slow adaptation" approximation is independent from α. On the other hand, when the neuron firing is more regular than a Poissonian spike train, as for strong potassium conductances g bringing the neuron well below the emission threshold for almost the whole ISI, the relative width of c distribution is independent from $v\ \tau_c$. This is why the limit of small coefficient of variation of c implies also a not too strong calcium feedback.

In such a limit, the density $p(v, c, t)$ then collapses in a one-dimensional subspace parallel to the v direction in Fig. 2. The flux $\mathbf{S}(v, c, t)$ gets a vanishing c component and the FP equation becomes:

$$\partial_t p(v, t) = -\partial_v \mu(v, t) p(v, t) + \frac{1}{2}\sigma^2 \partial_v^2 p(v, t) \tag{2.5}$$

where now $\mu(v,t) = -f(v) - g\ c(t) + \mu_{\text{ext}}(t)$

In this approximation $v(t) = v(c,t)\delta(c - c(t))$:

$$v(t) = -\frac{1}{2}\sigma^2 \partial_v p(v,t)|_{v=\theta} \tag{2.6}$$

As a result of the above dimensional reduction, the relevant boundary conditions will be those appropriate for $p(v,t)$, which are the same as for $p(v,c,t)$ neglecting the jumps α for c. For simplicity from now on α is set to 1.

2.3. Spectral decomposition of the FP operator

We can rewrite Eq. (2.5) as $\partial_t p = \mathcal{L}p$ defining the FP operator:

$$\mathcal{L} = -\partial_v \mu(v,t,c)\cdot + \frac{1}{2}\sigma^2 \partial_v^2 \tag{2.7}$$

Let us suppose a complete set of eigenfunctions for the FP operator $\mathcal{L}$ exists, with their associated eigenvalues:

$$\mathcal{L}\varphi_n(v) = \lambda_n \varphi_n(v)$$

where φs and λs will actually depend on μ, c and σ^2 as $\mathcal{L}$ itself. Defining the following inner product:

$$\langle \psi | \varphi \rangle \doteq \int \psi(v)\varphi(v)\mathrm{d}v \tag{2.8}$$

the adjoint of the FP operator:

$$\langle \psi | \mathcal{L}\varphi \rangle = \langle \mathcal{L}^+ \psi | \varphi \rangle \tag{2.9}$$

will have eigenfunctions and eigenvalues:

$$\mathcal{L}^+ \psi_n(v) = \lambda_n \psi_n(v)$$

$\mathcal{L}$ and $\mathcal{L}^+$ share the same set of eigenvalues as Eq. (2.9) implies that eigenfunctions with different eigenvalues are orthogonal and because of the assumed completeness of the φs. With an appropriate normalization the two sets of eigenfunctions are biorthonormal:

$$\langle \psi_n | \varphi_m \rangle = \delta_{nm} \tag{2.10}$$

Again because of completeness, φs will satisfy the same boundary conditions as $p(v,t)$ in Eq. (2.5).

Finally, it can be proven that [13,6]:

- the λs appear in general in complex conjugate pairs (this comes from the condition of reentering flux at H, as, without that condition, $\mathcal{L}$ would admit only real eigenvalues);
- the λs have negative real parts;
- always exists a $\lambda_0 = 0$ that correspond to the stationary solution of Eq. (2.5) (for μ, c and σ^2 kept fixed);

Please cite this article in press as: G. Gigante et al., Frequency-dependent response properties ..., Math. Biosci. (2006), doi:10.1016/j.mbs.2006.11.010

- $\psi_0(v) \equiv 1$.

2.4. Emission rate equation

Knowing the complete spectrum of the FP operator, we can expand every acceptable probability density function of v as:

$$p(v,t) = \sum_n a_n(t)\varphi_n(v) \tag{2.11}$$

for adequate coefficients $a_n(t)$. From this equation, using the orthonormality property (Eq. (2.10)) and the FP Eq. (2.5), we can derive a dynamics for the infinite set of as. Starting from:

$$a_n(t) = \langle \psi_n | p \rangle$$

and taking time derivatives we obtain:

$$\begin{aligned} \dot{a}_n(t) &= \langle \psi_n | \partial_t p \rangle + \langle \partial_t \psi_n | p \rangle = \langle \psi_n | \mathcal{L} p \rangle + \sum_k a_k \langle \partial_t \psi_n | \varphi_k \rangle \\ &= \langle \mathcal{L}^\dagger \psi_n | p \rangle + \sum_k a_k \langle \partial_\mu \psi_n | \varphi_k \rangle \dot{\mu} \\ &= \lambda_n a_n + \sum_k a_k \langle \partial_\mu \psi_n | \varphi_k \rangle \dot{\mu} \end{aligned} \tag{2.12}$$

We adopt in the following a matrix notation and write a_n for $n \neq 0$ as a vector, $\mathbf{a}$; since $\langle \psi_0 | p \rangle = \langle 1 | p \rangle = 1$ at any time (see Section 2.4), $a_0(t) \equiv 1$.

Then, we define the three following (infinite) matrices:

$$\Lambda_{nm} \equiv \delta_{nm}\lambda_n \tag{2.13}$$

$$M_{nm} \equiv \langle \partial_\mu \psi_n | \varphi_m \rangle \tag{2.14}$$

for $n, m \neq 0$, and the (infinite) vector:

$$m_n \equiv \langle \partial_\mu \psi_n | \varphi_0 \rangle \tag{2.15}$$

for $n \neq 0$.

With the help of these definitions, the set of Eqs. (2.12) can be restated as:

$$\begin{cases} \dot{\mathbf{a}} = (\Lambda + M\dot{\mu}(t))\mathbf{a} + \mathbf{m}\dot{\mu}(t) \\ a_0 = 1 \end{cases} \tag{2.16}$$

The set of Eq. (2.16) has to be complemented by a dynamic equation for c, which will in turn depend on $p(v,t)$ (that is on $\mathbf{a}$) through v, thus making the FP equation non-linear.

In order to close the loop, thanks to Eq. (2.11) we rewrite Eq. (2.6) as:

$$v(t) = -\frac{1}{2}\sigma^2(t)\partial_v p(v,t)|_{v=0} = -\frac{1}{2}\sigma^2(t)\sum_n a_n(t)\partial_v \varphi_n(v,t)|_{v=0} \tag{2.17}$$

Defining:

$$\Phi(\mu,\sigma) \doteq -\frac{1}{2}\sigma^2(t)\partial_v \varphi_0(v,t)|_{v=0} \tag{2.18}$$

(Φ is the mean emission rate of the neuron in stationary condition, again for μ, c and σ^2 kept fixed) and:

$$f_n(\mu,\sigma)\doteq -\frac{1}{2}\sigma^2(t)\partial_v\varphi_n(v,t)|_{v=\theta} \tag{2.19}$$

for $n \neq 0$ and writing all the f_n as a vector, $\mathbf{f}$, we can rewrite Eq. (2.17) as:

$$\nu(t) = \Phi + \mathbf{f}\cdot\mathbf{a} \tag{2.20}$$

recalling that $a_0 \equiv 1$.

Now we are done: we reduced our problem, thanks to an adiabatic approximation and a spectral expansion of the FP operator, to the solution of the following dynamical system:

$$\begin{cases} \dot{\mathbf{a}} = (\Lambda + M\dot{\mu}(t))\mathbf{a} + \mathbf{m}\dot{\mu}(t) \\ \nu = \Phi + \mathbf{f}\cdot\mathbf{a} \\ \dot{c} = -c/\tau_c + \nu \end{cases} \tag{2.21}$$

The solution of this infinite set of equations is not, generally, easier than that of the original problem; one advantage of this formulation is that Eqs. (2.21) are much more amenable to approximate treatments than Eqs. (2.4) and (2.5).

2.5. A finite set of neurons

The total emission rate per neuron of a finite *ensemble* of neurons will always present random fluctuations around the average $\nu(t)$. Such fluctuations have a special interest since, as we will see in a moment, they provide much information about the frequency response of the single neuron. Indeed, even if we are discussing the behavior of a set of independent spiking neurons the emerging spectral properties will be of course single cell properties, but in order to consider the presented theoretical framework as a first step toward the analysis of network of neurons with adaptation, we follow the approach introduced in [14,6].

Consider a homogeneous population of N independent neurons (that is not connected by synaptic couplings). Let us focus our attention on a small time interval $\mathrm{d}t$, and count the number $\mathrm{d}n_N$ of spikes emitted by the population in that interval, which will be approximately a Poisson variable, with mean and variance $N\nu(t)\mathrm{d}t$. The instantaneous emission rate of the *finite* population $\nu_N(t)$ is estimated by:

$$\nu_N(t)\doteq\frac{1}{N}\frac{\mathrm{d}n_N(t)}{\mathrm{d}t} \tag{2.22}$$

As long as $N\nu(t)\mathrm{d}t \gg 1$, $\mathrm{d}n_N$ can be again well approximated by a Gaussian variable; since there are no correlations between successive $\mathrm{d}n_N$, for $\mathrm{d}t$ smaller than any time scale of the dynamics, we can write $\nu_N(t)$ as:

$$\nu_N(t)\doteq\nu(t)+\sqrt{\frac{\nu(t)}{N}}\Gamma(t) \tag{2.23}$$

where $\Gamma(t)$ is a standard white-noise. As one could expect, for $N\to\infty$, $\nu_N(t)\to\nu(t)$.

Please cite this article in press as: G. Gigante et al., Frequency-dependent response properties ..., Math. Biosci. (2006), doi:10.1016/j.mbs.2006.11.010

In order to describe the dynamics of $v_N(t)$, we recall two main points in the FP description of our system. First, $v(t)$ represents the probability flux through the emission threshold θ; second, this flux reenters instantaneously at the reset potential H: this is the analytical counterpart of the resetting after the emission of a spike. Thus, fluctuations in $v_N(t)$ will be immediately felt at H. This effect can be incorporated in the FP description defining a new finite-size, stochastic FP operator:

$$\mathcal{L}_N \doteq \mathcal{L} + \delta(v - H)\sqrt{\frac{v(t)}{N}}\Gamma(t) \tag{2.24}$$

which corresponds to an *emission rate equation* for $v_N(t)$, that reads:

$$\begin{cases} \dot{\mathbf{a}} = (\Lambda + M\dot{\mu}(t))\mathbf{a} + \mathbf{m}\dot{\mu}(t) + \boldsymbol{\psi}\sqrt{v/N}\Gamma(t) \\ v_N = \Phi + \mathbf{f}\cdot\mathbf{a} + \sqrt{v/N}\Gamma(t) \equiv v + \sqrt{v/N}\Gamma(t) \\ \dot{c} = -c/\tau_c + v_N \end{cases} \tag{2.25}$$

where the vector $\boldsymbol{\psi}$ has elements $\psi_k(H)$, where $\psi_k(v)$ is the eigenfunction of $\mathcal{L}^+$ with eigenvalue λ_k. The additional term on the r.h.s. in the first equation comes directly from the δ-function appearing in $\mathcal{L}_N$.

2.6. Fixed points and local analysis

In the limit $N \to \infty$ and in absence of non-stationary external stimulations, the system may relax to fixed points such that $\dot{\mathbf{a}} = 0$, $c\cdot = 0$ and $\dot{v} = 0$, solutions of:

$$\{\mathbf{a}_0 = 0, v_0 = \Phi(c_0), c_0 = v_0\tau_c\} \tag{2.26}$$

The non-linear Eq. (2.21) can be then linearized around such fixed points to study small perturbations due to external non-stationary stimulations or the finite-size fluctuations of the emission rate. To do that we introduce the displacements from the fixed point $v_1(t) \doteq v(t) - v_0$, $c_1(t) \doteq c(t) - c_0$ and $\mathbf{a}(t)$. Neglecting terms of order higher than the first the emission rate equation reduces to:

$$\begin{cases} \dot{\mathbf{a}} = \Lambda\mathbf{a} + \mathbf{m}_0\dot{\mu}_1 + \boldsymbol{\psi}_0\sqrt{v_0/N}\Gamma(t) \\ v_1 = \Phi_\mu\mu_1 + \mathbf{f}_0\cdot\mathbf{a} + \sqrt{v_0/N}\Gamma(t) \\ \dot{c}_1 = -c_1/\tau_c + v_1 \end{cases} \tag{2.27}$$

where all the functions are calculated at the fixed point, including $\Phi_\mu \doteq \partial_\mu\Phi(\mu, \sigma^2)$. In particular $\mu_1(t) \doteq \mu(t) - g\,c_0 - \beta + \mu_{ext}$ is the perturbation of the infinitesimal mean due to the fluctuation of c and the possible external stimulation.

3. Spectral analysis

A finite set of uncoupled identical neurons may provide a train of spikes exhibiting a rich repertoire of resonances. Performing the Fourier transform $v_1(\omega)$ of the population emission rate

from the linearized Eq. (2.27), the spectral properties of the system can be studied by means of the power spectrum $P_1(\omega) = |\nu_1(\omega)|^2$:

$$P_1(\omega) = \frac{1 + 2\mathrm{Re}\left[\mathbf{f}_0 \cdot (\mathrm{i}\omega I - \Lambda_0)^{-1}\boldsymbol{\psi}_0\right]}{|1 - \frac{g\tau_c}{1+\mathrm{i}\omega\tau_c}\left[\Phi_\mu + \mathrm{i}\omega\mathbf{f}_0 \cdot (\mathrm{i}\omega I - \Lambda_0)^{-1}\mathbf{m}_0\right]|^2} \frac{\nu_0}{N} \tag{3.1}$$

where we have considered only the first order term in the finite-size fluctuation size [7]. Some features emerge: (i) for high ω, $P_1(\omega)$ approaches the white noise flat spectrum due to the superposition of the δs composing the spike train and (ii) when the eigenvalues λ_k are complex conjugate damped resonances appear at frequencies $\omega \simeq \mathrm{Im}\,\lambda_k$, where $\mathrm{i}\omega I - \Lambda_0$ attains a local minimum.

In Eq. (3.1) are recognizable the different terms due to the finite-size fluctuations (numerator), the membrane potential integration and the self-inhibition related to the calcium dynamics (the product in the denominator). This power spectrum shape is quite general for linear systems with recurrent inhibition. Indeed, similar results has been reported for networks of synaptically connected inhibitory neurons [7,15], showing the ability of these kind of systems to distribute the 'input–output channel' noise on different Fourier frequency bands [16,17,7].

In Fig. 3 we plot the estimated power spectrum, averaged over 25 runs of $N = 5000$ independent neurons (diamonds; gray shades indicate standard errors); in this case we have $\tau_c = 500$ ms. On the same plot (solid line) the theoretical prediction Eq. (3.1) is drawn, showing a remarkable agreement with simulation results.

The main features of $P_1(\omega)$ are well represented in this plot. For large ω, the power spectrum approaches the asymptotic value ν_0/N: from Eq. (2.23) it is seen that, whatever the (inevitably finite) ω-content of ν, the flat contribution of the white noise will ultimately dominate for sufficiently high ω.

$P_1(\omega)$ shows also a clear resonance centered at $\omega/2\pi \simeq 5\ Hz = \nu_0$; indeed, when neurons, as in this case, are in a small-σ regime (i.e. when the deterministic component of the afferent current

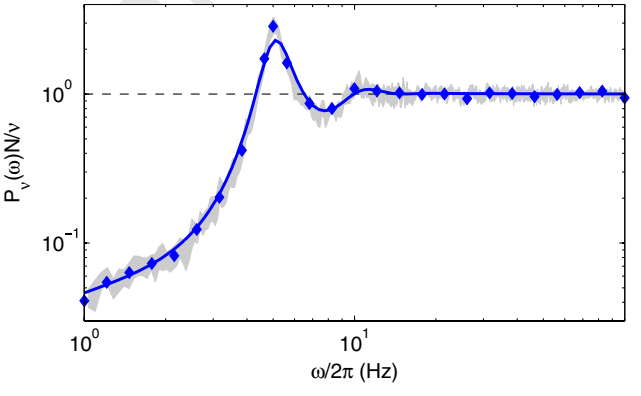

Fig. 3. Power spectrum of finite-size emission rate ν_N in stationary state estimated from simulation (diamonds) with errors (gray shades) against the theoretical prediction $P_1(\omega)$ given by Eq. (3.1) (solid line), computed using 2048 couples of eigenfunctions. The neuron parameters are $\beta = 50\theta$/s, $H = 0$, $\mu_{\mathrm{ext}} = 4.87\theta$/s, $\sigma^2_{\mathrm{ext}} = 0.25\theta^2$/s, $g = 1\theta$/s, $\tau_c = 0.5$ s. The power spectrum was estimated from 25 runs of $N = 5000$ neurons lasting 105 s, neglecting a transient period of 5 s; the sampling frequency was 2 kHz.

Please cite this article in press as: G. Gigante et al., Frequency-dependent response properties ..., Math. Biosci. (2006), doi:10.1016/j.mbs.2006.11.010

alone is enough to make the neurons fire), $|\mathrm{Im}\,\lambda_{\pm 1}| \simeq 2\pi\nu_0$. Under this condition, random clusters of neurons which happen to fire roughly at the same time evolve together in a quasi-deterministic way, providing quasi-periodic bumps of activity at the same frequency as the single neuron firing rate; this accounts for $|\mathrm{Im}\,\lambda_{\pm 1}|$ being close to $2\pi\nu_0$, and then for the resonances appearing in the power spectrum, previously described in [18,19,6].

Fig. 4 shows $P_1(\omega)$ for increasing levels of SFA and $\tau_c = 250$ ms; markers: simulations results, continuous lines theoretical predictions. The plot shows that a major effect of SFA on the resonant properties is to decrease power at low frequencies; such decrease is more marked as SFA gets stronger (increasing g, see Eq. (2.1)). In other words, SFA acts on the emission rate dynamics as a *high-pass filter* [20].

Such behavior is, in a sense, counterintuitive since the calcium dynamics acts exactly as a *low-pass filter* on $\nu(t)$ (see third equation in (2.21)). The explanation is found in the negative feedback occurring between the emission rate ν and the calcium variable c. Indeed, c will actually filter the high-ω components of the emission rate; in turn, the power associated with the low-ω components of ν surviving the filter cut, will be available for SFA damping, which will be self-consistently more efficient on the low-ω components of ν, thereby digging a hole in the low-ω part of $P_1(\omega)$.

In other words, SFA will not be able to cut off rapid variations of ν, because c has not time enough to build up, and then to inhibit those variations; on the other hand, a slow component of ν will elicit a strong response by calcium dynamics, and therefore a strong inhibitory current that will tend to shut it off. This same reasoning leads one to conclude that if τ_c is shortened, the effects of SFA on the power spectrum spread on a wider range of ω, since, roughly speaking, calcium dynamics is effective for $\omega < 1/\tau_c$.

Fig. 4 also shows how, increasing g, the theoretical prediction becomes ever less accurate. In this plot, the neuron is in a current regime particularly unfavorable for the adiabatic approxima-

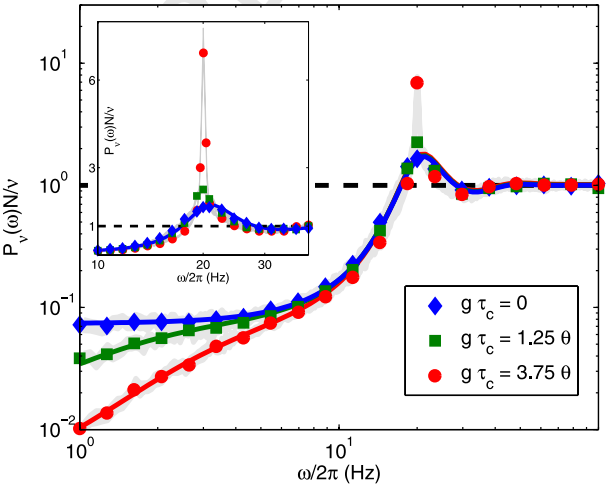

Fig. 4. Theoretical predictions Eq. (3.1) (continuous lines) and simulation results (markers) for the power spectrum of the finite-size emission rate ν_N in stationary conditions for different values of g and $\tau_c = 250$ ms. Theoretical predictions have been computed using 2048 couples of eigenfunctions. Inset: zoom, with linear y-scale, around the resonance at about 20 Hz.

Please cite this article in press as: G. Gigante et al., Frequency-dependent response properties ..., Math. Biosci. (2006), doi:10.1016/j.mbs.2006.11.010

tion, since in absence of SFA the neuron fires rather regularly, as demonstrated by the resonance at frequency $f \simeq 20$ Hz, that is about the single neuron emission rate. The greatest differences appear indeed close to this resonance, and the inset in Fig. 4 shows a zoom of the three power spectra around the peak (note that the y-scale is now linear); the theoretical prediction systematically undersimates the power of the resonance and is, for this range of ω, actually insensible to variations of g (blue line: theory for $g = 0$).

4. Response to oscillatory input

Coming back to the $N \to \infty$ case, we now undertake to study the adapting neuron dynamics under the influence of an oscillatory input current.

In [3] the authors studied, in experiment and in theory, the emission rate of an IF neuron with SFA (in a somewhat different model) in response to a gaussian current with a sinusoidally modulated mean with frequency ω. They found that the oscillatory response exhibits an amplitude modulation $\tilde{A}$ and phase shift φ with respect to the input, both dependent on ω. In particular, they demonstrated that the curve $\varphi(\omega)$ crosses the zero-phase-shift line ($\varphi = 0$) twice, one at $\omega = 0$ the other at a *preferred frequency* ω^*, which, the authors argued, has a leading role in setting up the frequency of collective global oscillations in networks of interacting adapting neurons.

In this section we will recover the results found in [3] using the theoretical framework set up in Section 2, with no need of additional assumptions. The curve $\varphi(\omega)$ can be computed in an interesting range of ω, ω^* is predicted and successfully checked against simulations.

4.1. Small time-scale approximation

With reference to Eqs. (2.27), for the sinusoidally modulated input we will have:

$$\mu_1(t) = A\sin(\omega t) - gc_1(t) \tag{4.1}$$

where A is small enough to fulfill the linear approximation hypothesis. Since we are not interested here in the finite-size effects, we neglect Γ terms. The solution of the linear, first order equation for $\mathbf{a}$ in the system Eq. (2.27) has the form:

$$\mathbf{a}(t) = \left[\int_{-\infty}^{t} \mathrm{e}^{-\Lambda_0(s-t)}\dot{\mu}_1(s)\mathrm{d}s\right]\mathbf{m}_0 \tag{4.2}$$

The latter equation can be rewritten, using integration by parts, as:

$$\begin{aligned}\int_{-\infty}^{t} \mathrm{e}^{-\Lambda_0(s-t)}\dot{\mu}_1(s)\mathrm{d}s = &-\dot{\mu}_1(t)\Lambda_0^{-1} - \cdots - \mu_1^{(k+1)}(t)\Lambda_0^{-(k+1)} \\ &+ \Lambda_0^{-(k+1)}\int_{-\infty}^{t} \mathrm{e}^{-\Lambda_0(s-t)}\mu_1^{(k+2)}(s)\mathrm{d}s\end{aligned} \tag{4.3}$$

Substitution of the above expansion into Eq. (4.2) gives:

$$\mathbf{a}(t) = -\left[\dot{\mu}_1\Lambda_0^{-1}\mathbf{m}_0 + \ddot{\mu}_1\Lambda_0^{-2}\mathbf{m}_0 + \cdots\right] \tag{4.4}$$

Please cite this article in press as: G. Gigante et al., Frequency-dependent response properties ..., Math. Biosci. (2006), doi:10.1016/j.mbs.2006.11.010

366 which, upon insertion into the second of Eqs. (2.27) results in:

368 $$v_1 = \tau_0\mu_1 - \tau_1\dot{\mu}_1 + \tau_2\ddot{\mu}_1 + \cdots \tag{4.5}$$

369 having defined:

371 $$\tau_k = (-1)^{k+1}\sum \frac{f_n m_n}{\lambda_n^k} \quad \text{for } k \geqslant 0 \tag{4.6}$$

372 This definition holds also for $k=0$ since it can be proved that $\Phi_\mu \equiv -\sum f_n m_n$. The series in the
373 above equations converge rapidly and only few couples of eigenfunctions and eigenvalues may
374 be taken into account for good numerical estimates.
375 Now we introduce an approximation by assuming that $\mu_1(t)$ is a 'slow' function with a typical
376 time scale τ_μ, much longer than the intrinsic time scales of **a** dynamics (i.e. Λ_0^{-1}). Under this
377 hypothesis, successive terms in Eq. (4.3) will be decreasing in magnitude, since the nth term of
378 the expansion will be of order $(\Lambda_0\tau_\mu)^{-n}$.
379 In the case of interest of an oscillatory input, $\tau_\mu = \omega^{-1}$. Since λ_1 (calculated at the fixed point) is
380 the eigenvalue with the smallest absolute value, the 'slowness' condition for $\mu_1(t)$ will simply read
381 $\omega \ll |\lambda_1|$, which allows us to truncate Eq. (4.5). In this way, using Eqs. (4.1) and the third of Eqs.
382 (2.27), Eq. (4.5) can be transformed to a kth order differential equation for v_1.
383 In [20] the authors have discussed the implications of SFA on the spectral properties of neu-
384 rons, in a zeroth order approximation, that is assuming the v dynamics instantaneous or, in
385 our notation, keeping only τ_0 terms. Our approach allows to consider higher order terms, and thus
386 to describe the system behavior with greater detail. For example, stopping at $k = 1$ in Eq. (4.5), we
387 have:

389 $$v_1(1 - g\tau_1) = A[\tau_0 \sin(\omega t) - \tau_1\omega\cos(\omega t)] - gc_1\left[\tau_0 + \frac{\tau_1}{\tau_c}\right] \tag{4.7}$$

390 Now, deriving both sides:

392 $$\dot{v}_1(1 - g\tau_1) = A\left[\omega\tau_0\cos(\omega t) + \omega^2\tau_1\sin(\omega t)\right] - g\dot{c}_1\left[\tau_0 + \frac{\tau_1}{\tau_c}\right] \tag{4.8}$$

393 Using Eq. (2.27) for $c\cdot_1(t)$, the preceding equation becomes:

395 $$\dot{v}_1(1 - g\tau_1) = A\left[\omega\tau_0\cos(\omega t) + \omega^2\tau_1\sin(\omega t)\right] - g\left(-\frac{c_1}{\tau_c} + v_1\right)\left[\tau_0 + \frac{\tau_1}{\tau_c}\right] \tag{4.9}$$

396 Finally, using Eq. (4.7) to substitute c_1, we get the first-order dynamics, for $g \neq 0$:

398 $$\dot{v}_1 = -\frac{v_1}{1 - g\tau_1}\left(\frac{1}{\tau_c} + g\tau_0\right) + \frac{A}{1 - g\tau_1}\left[\omega(\tau_0 - \frac{\tau_1}{\tau_c})\cos(\omega t) + (\tau_1\omega^2 + \frac{\tau_0}{\tau_c})\sin(\omega t)\right] \tag{4.10}$$

399 which has the asymptotic solution:

401 $$v(t) = v_0 + \tilde{A}(\omega)\sin(\omega t - \varphi(\omega)) \tag{4.11}$$

402 Left panel in Fig. 5 shows the amplitude of the sinusoidal component $\tilde{A}(\omega)$ of v; a good agreement
403 is achieved on the considered range of ω between simulation result (blue squares) and third order
404 theory (continuous blue line). The plot clearly shows how the neuron acts as a *band-pass filter* on

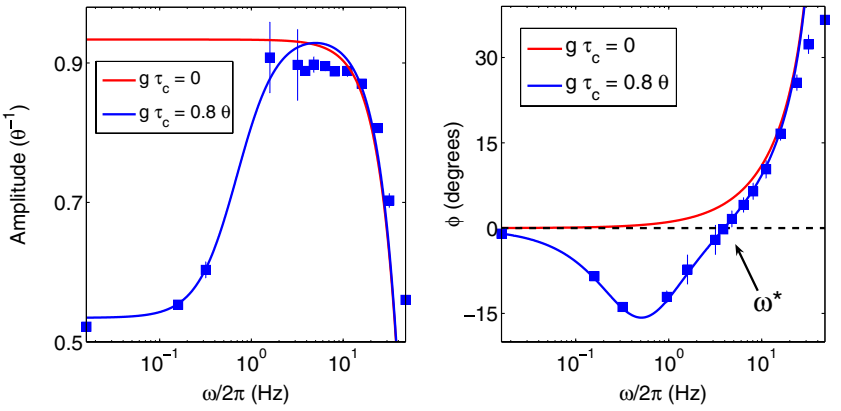

Fig. 5. Band-pass and phase-locking properties of adapting neuron: amplitude (left panel) and phase shift (right panel) of the oscillatory component of $v(t)$. The squares mark the values estimated from simulations (vertical bars represent standard errors), whereas the continuous blue line is the theoretical prediction truncated at order $k = 3$. The red lines show the theoretical prediction for $g = 0$.

small sinusoidal inputs [20]. This behavior is mainly due to the interplay between v and c dynamics. The first one accounts for the high frequency cutoff, as discussed above. On the other hand, as we have seen in Section 3, SFA acts partially as a high pass filter on v, damping any slow component of the emission rate. The overall result is a bell-shaped amplitude $\tilde{A}(\omega)$ for the neuron response. The role of SFA is better understood looking at the red continuous line of Fig. 5 that shows the neuron response amplitude (theoretical prediction) for $g = 0$, i.e. in absence of adaptation; for low ω, SFA leads to a sensible decrease in power with respect to the $g = 0$ case, whereas, for higher ω, the two lines tend to overlap, since the slow calcium dynamics is no more effective at that frequencies.

Right panel in Fig. 5 shows the phase shift $\varphi(\omega)$; the agreement between simulation (blue squares) and theory (continuous blue line) is good in the considered range of ω. In particular, the preferred angular frequency ω^* is well predicted; higher k terms ensure good estimates for higher ω. The phase shift is negative for $\omega < \omega^*$ and positive for $\omega > \omega^*$; in other words, for low frequencies of the oscillatory input current, the neuron response is anticipated with respect to the stimulus, whereas for higher ω it is delayed. For $\omega \to 0^+$, the stimulus and the emission rate are trivially phase-locked.

The red line, on the other hand, shows the theoretical phase shift for $g = 0$; in this case $\varphi(\omega)$ is always greater than zero. In order to have phase-locking a finite g is in fact needed. Indeed, deriving Eq. (4.5), keeping only first order terms, one gets:

$$\dot{\mu}_1 = \frac{\dot{\nu}_1}{\tau_0} - \frac{\tau_1}{\tau_0}\ddot{\mu}_1 \tag{4.12}$$

Inserting this result again in Eq. (4.5), and neglecting the $\ddot{\mu}_1$ term, since its order is greater than one, one obtains:

$$\tau^* \dot{\nu}_1 = -\nu_1 + \tau_0 \mu_1 \tag{4.13}$$

with $\tau^* \doteq \tau_1/\tau_0$. This is a first order differential equation for v_1; since it describes a physical system, τ^* (and therefore τ_1, since $\tau_0 = \Phi_\mu > 0$) must be positive in order not to have exploding solutions for any small (and slow) μ_1. Such equation implies a positive phase shift for every ω.

It is interesting to note that, truncating expansion Eq. (4.5) to τ_1, ω^* takes a simple explicit form:

$$\omega^* = \frac{1}{\tau_c}\sqrt{\frac{g\Phi_\mu^2\tau_c^2 - \tau_1}{\tau_1(1 - g\tau_1)}} \simeq \sqrt{\frac{g\Phi_\mu^2}{\tau_1}} + O(1) \quad \text{for } \tau_1 \to 0 \tag{4.14}$$

This equation clearly shows that for $g \to 0^+$, ω^* can take imaginary values, that have no physical meaning; in addition, one has that:

$$\varphi(\omega) \simeq \frac{\tau^* - g\tau_c^2\Phi_\mu}{1 + g\tau_c\Phi_\mu}\omega \quad \text{for } \omega \to 0^+ \tag{4.15}$$

therefore, for small $\omega, \varphi(\omega)$ is negative only if ω^* is real, that is when $g > \tau^*/\tau_0\tau_c^2$. This result strongly suggests that below a given SFA level, v_1 can never 'anticipate' its input.

The first order approach, thence, allows to predict phase-locking properties of the system, that a zeroth order one (see [20]) cannot derive.

The limit $\tau_1 \to 0^+$ in Eq. (4.14) is relevant since τ_1 is very small for typical parameters. The leading order of the expansion for small τ_1 has the same form as the expression found for ω^* in [3], with the bonus of no free parameters. Writing the leading term in Eq. (4.14) as:

$$\omega^* \simeq \sqrt{\frac{1}{\tau^*}}\sqrt{g\Phi_\mu} \tag{4.16}$$

we can distinguish in ω^* two contributions. The first one is related to τ^*, the characteristic time scale of the neuron relaxation dynamics; the other term is $g\Phi_\mu = -\partial_c\Phi$, that measures the sensitivity of the stationary emission rate to changes in the calcium concentration, and acts as the elastic force term of the damped oscillator.

5. Conclusions

The approach to the population density formalism introduced in [6] has been extended to account for the implications of SFA. In the present work we dealt with (1) the effects of sampling a finite number of identical, adapting neurons, on the structure of the power spectrum of their total measured firing rate; (2) the response properties of (an infinite sample of) adapting neurons to an oscillatory input, with special reference to phase-locking and band-pass properties.

The formalism extends naturally to the case of synaptically coupled adapting neurons, which will be reported elsewhere [21].

Acknowledgement

This work has been supported by the ALAVLSI EU grant IST-2001-38099.

Please cite this article in press as: G. Gigante et al., Frequency-dependent response properties ..., Math. Biosci. (2006), doi:10.1016/j.mbs.2006.11.010

References

[1] A. Treves, Mean-field analysis of neuronal spike dynamics, Network 4 (1993) 259–284.
[2] Y.H. Liu, X.J. Wang, Spike-frequency adaptation of a generalized leaky integrate-and-fire model neuron, J. Comput. Neurosci. 10 (1) (2001) 25–45.
[3] G. Fuhrmann, H. Markram, M. Tsodyks, Spike frequency adaptation and neocortical rhythms, J. Neurophysiol. 88 (2) (2002) 761–770.
[4] A. Rauch, G. La Camera, H.-R. Lüscher, W. Senn, S. Fusi, Neocortical pyramidal cells respond as integrate-and-fire neurons to in vivo-like input currents, J. Neurophysiol. 90 (3) (2003) 1598–1612.
[5] B.W. Knight, D. Manin, L. Sirovich, Dynamical models of interacting neuron populations in visual cortex, in: E.C. Gerf (Ed.), Proc. of SRC, Lille-France, 1996.
[6] M. Mattia, P. Del Giudice, Population dynamics of interacting spiking neurons, Phys. Rev. E 66 (5 Pt. 1) (2002) 051917.
[7] M. Mattia, P. Del Giudice, Finite-size dynamics of inhibitory and excitatory interacting spiking neurons, Phys. Rev. E 70 (5 Pt. 1) (2004) 052903.
[8] C.A. Mead, Analog VLSI and neural systems, Addison Wesley, Reading, MA, 1989.
[9] S. Fusi, M. Mattia, Collective behavior of networks with linear (VLSI) integrate-and-fire neurons, Neural Comput. 11 (3) (1999) 633–653.
[10] H.C. Tuckwell, Introduction to Theoretical Neurobiology, vol. 2, Cambridge University Press, Cambridge, 1988.
[11] N. Brunel, F.S. Chance, N. Fourcaud, L.F. Abbott, Effects of synaptic noise and filtering on the frequency response of spiking neurons, Phys. Rev. Lett. 86 (10) (2001) 2186–2189.
[12] X.-J. Wang, Synaptic basis of cortical persistent activity: the importance of nmda receptors to working memory, J. Neurosci. 19 (1999) 9587–9603.
[13] B.W. Knight, Dynamics of encoding in neuron populations: some general mathematical features, Neural Comput. 12 (3) (2000) 473–518.
[14] N. Brunel, V. Hakim, Fast global oscillations in netwoks of integrate-and-fire neurons with low firing rates, Neural Comput. 11 (1999) 1621–1671.
[15] B. Lindner, B. Doiron, A. Longtin, Theory of oscillatory firing induced by spatially correlated noise and delayed inhibitory feedback, Phys. Rev. E 72 (6 Pt. 1) (2005) 061919.
[16] D.J. Mar, C.C. Chow, W. Gerstner, R.W. Adams, J.J. Collins, Noise shaping in populations of coupled model neurons, Proc. Natl. Acad. Sci. USA 96 (1999) 10450–10455.
[17] M.J. Chacron, B. Lindner, A. Longtin, Noise shaping by interval correlations increases information transfer, Phys. Rev. Lett. 92 (8) (2004) 080601.
[18] B.W. Knight, Dynamics of encoding in a population of neurons, J. Gen. Physiol. 59 (1972) 734–766.
[19] R.B. Stein, A.S. French, A.V. Holden, The frequency response, coherence, and information capacity of two neuronal models, Biophys. J. 12 (1972) 295–322.
[20] J. Benda, A.V. Herz, A universal model for spike-frequency adaptation, Neural Comput. 15 (11) (2003) 2523–2564.
[21] G. Gigante, M. Mattia, P. Del Giudice, Diverse population bursting modes of adapting spiking neurons, submitted for publication.

Please cite this article in press as: G. Gigante et al., Frequency-dependent response properties ..., Math. Biosci. (2006), doi:10.1016/j.mbs.2006.11.010